The Performance of Wind Turbine Smart Rotor Control Approaches During Extreme Loads

Matthew A. Lackner and Gijs van Kuik

November 3, 2008

Abstract

Reducing the loads experienced by wind turbine rotor blades can lower the cost of energy of wind turbines. "Smart rotor control" concepts have emerged as a solution to reduce fatigue loads on wind turbines. In this approach, aerodynamic load control devices are distributed along the span of the blade, and through a combination of sensing, control, and actuation, these devices dynamically control the blade loads. While smart rotor control approaches are primarily focused on fatigue load reductions, extreme loads on the blades may also be critical in determining the lifetime of components, and the ability to reduce these loads as well would be a welcome property of any smart rotor control approach. This research investigates the extreme load reduction potential of smart rotor control devices, namely trailing edge flaps (TEFs), in the operation of a 5 MW wind turbine. The controller utilized in these simulations is designed explicitly for fatigue load reductions; nevertheless its effectiveness during extreme loads is assessed. Simple step functions in the wind are used to approximate gusts and investigate the performance of two load reduction methods, individual flap control and individual pitch control. Both local and global gusts are simulated, as well as safety system situations. The results yield important insight into the control approach that is utilized, and also into the differences between using individual pitch control and trailing edge flaps for extreme load reductions. Finally, the limitation of the assumption of quasi-steady aerodynamic behavior is assessed.

Nomenclature

C_D	Coefficient of Drag
C_L	Coefficient of Lift
C_M	Coefficient of Pitching Moment
$DEQL$	Damage Equivalent Load
$DTEG$	Deformable Trailing Edge Geometry
IFC	Individual Flap Control
IPC	Individual Pitch Control
k	Reduced Frequency
kWh	Kilowatt-Hour
LTI	Linear Time Invariant

LTV	Linear Time Varying
M_y	Blade Root Flapwise Bending Moment
PID	Proportional-Integral-Derivative
SC	Standard Control
$SISO$	Single Input Single Output
TUD	Technical University of Delft
TEF	Trailing Edge Flap
α	Angle of Attack

1 Introduction

Wind turbines are subjected to significant and rapid fluctuating loads, which arise from a variety of sources including: turbulence in the wind, tower shadow, wind shear, yawed flow, and gusts. Fatigue loads can lead to damage of turbine components and eventually to failures. "Smart rotor control" concepts have emerged as a possible means to reduce fatigue loads on wind turbines. In this approach, aerodynamic load control devices are distributed along the span of the blade, and through a combination of sensing, control, and actuation, these devices dynamically control the loads on the blades, at any azimuthal position. Previous research presented by the authors has focused on utilizing smart rotor control approaches for reducing blade fatigue loads [1].

The research presented here focuses on a distinct, but complimentary problem: the potential to utilize smart rotor control approaches for reducing extreme loads due to gusts and safety system situations. While the reduction of fatigue loads is the primary objective of smart rotor control approaches such as individual pitch control (IPC) and individual flap control (IFC), the ability to reduce the damage due to extreme loads could be an important secondary property of any approach. Both fatigue loads and extreme loads contribute to the accrued damage in turbine components that eventually leads to failures. Load control devices and smart rotor control approaches that can reduce both types of loads may be especially advantageous and lead to significantly increased lifetimes of components or reduced costs. This research investigates the issue of extreme loads by simulating the operation of a 5 MW turbine equipped with trailing edge flaps in an aero-elastic design code, GH Bladed.

1.1 Previous Work

Smart rotor control has become an active area of research for wind turbine applications [2]. Barlas provides detailed summaries of smart rotor control research for wind turbines, including thorough reviews of potential actuators, sensors, aerodynamic control surfaces, control approaches, and simulation environments [3].

Individual pitch control is a popular potential smart rotor control concept, and several investigations into the use of IPC schemes have been conducted recently. van Engelen and van der Hooft [4], Bossayni [5], and Selvam [6], along with others, have

investigated control approaches for IPC, simulated IPC schemes, and demonstrated sizable load reduction capabilities of the IPC approach.

Smart rotor control simulations that utilize localized load control devices have also been conducted. In particular, the work of Andersen et al. [7], and McCoy and Griffin [8] simulate spanwise distributed load control devices, and provide a useful comparison to this research. Other similar research includes the work of Zayas et al. [9]. In general, these investigations focus exclusively on fatigue loads during turbulent wind simulations, and not on extreme loads.

2 Modeling and Procedure

2.1 Turbine Model and Simulation Environment

The simulation of a 5 MW wind turbine with controllable trailing edge flaps is carried out using the aero-elastic simulation package GH Bladed. Some of the important features that Bladed provides are:

- Aerodynamics are calculated using the well-known Blade Element-Momentum (BEM) approach. Dynamic inflow and dynamic stall models are also incorporated to model the turbine wake and deal with unsteady aerodynamic conditions.
- The structural dynamics of the turbine model are calculated using a limited degree of freedom modal model.
- The dynamics of the power train (shaft, gearbox, and generator) are modeled.
- The external wind conditions can be generated, including 3D turbulent wind fields, wind shear, tower shadow effects, and prescribed gusts.
- Control of the turbine can be accomplished using either internal controller provide by Bladed, or external controllers written by the user can be incorporated.
- The loads on the various components of the turbine and the turbine performance are calculated.

The wind turbine model used for the analysis in Bladed is the NREL 5 MW (also referred to as the UpWind 5 MW) wind turbine [10]. The turbine is a horizontal axis, 3 bladed, upwind, variable speed, pitch controlled turbine, with a 126 m rotor diameter, 90 m hub height, and 20 m water depth.

Bladed is capable of including trailing edge flaps in the turbine model, and allows the TEFs to operate concurrently with variable speed, pitch controlled operation. The TEFs are added to the blade planform from 70% to 90% span. The TEFs are chosen to have a chordwise length of 10% and a deflection range of ± 10 degrees. These dimensions and deflection ranges are chosen partially based on the work of Troldborg, who investigated the effectiveness of trailing edge flaps for a variety of configurations [11].

The aerodynamic performance of the TEFs are determined using XFOIL 6.9, which is a 2D viscous panel code [12]. XFOIL is used to generate the coefficients of lift, drag,

and pitching moment as a function of angle of attack, for TEF deflection angles ranging from -10 degrees to 10 degrees in 1 degree increments. A Reynolds number of 6 million is used for these calculations.

2.2 Turbine Control

External controllers, written in Fortran and compiled as .dll files, are used to control the wind turbine model in Bladed. These external controllers control the generator torque, blade pitch, and TEF deployment angles.

2.2.1 Standard Control

A baseline controller for the wind turbine model is provided by NREL. This is the "standard controller" for the NREL/UpWind 5 MW turbine model, and so it controls the generator torque and collective blade pitch, but does not control the TEFs. The generator torque control is a quadratic function of the generator speed in region 2 for optimal tip speed ratio operation. In region 3, the generator torque is used to produce constant power output of the turbine. The collective blade pitch is also used to control the rotor speed in region 3, with a basic PID controller.

2.2.2 Load Reduction Controller Design

A load reduction controller, used for both individual flap control (IFC) and individual pitch control (IPC), is developed with the specific goal of reducing the fatigue loads. Fatigue load reduction is the primary goal of the smart rotor approach, and so not surprisingly the controller is designed with this goal in mind. On the other hand, wind turbines also operate during gusts and must undergo safety system situations such as stoppages, and so these same load reduction controllers may operate under these extreme situations as well. While this research is concerned with extreme due to gusts and transients, the control approach that is developed for reducing fatigue loads is not changed; instead, the ability of these smart control approaches operating based on the fatigue load reduction control approach, is assessed when extreme events occur. Thsu, the fatigue load reduction controller is now described, and is utilized throughout the simulations presented in this paper.

Broadly, the goal of the load reduction control approach is to affect the blade root flapwise bending moment of each of the three blades (M_{y1}, M_{y2}, and M_{y3}), by adjusting either the TEFs or the blade pitch angles. The major challenge in implementing this feedback control approach is due to the fact that the blades are in a rotating coordinate system, and so the equations of motion that relate M_{y1}, M_{y2}, and M_{y3} and the TEFs or blade pitch contain periodic coefficients. The result is a linear time varying ("LTV") system.

The issue of a rotating coordinate system has been identified numerous times in smart rotor control research [4],[5],[6],[8],[13]. The most common solution is a multi-blade transformation, or Coleman transformation, which maps the individual blade variables in the rotating frame of reference into a fixed reference frame [14]. While it is not

precisely true, it can be assumed that the transformed system is time invariant and so LTI control techniques can be used [4],[6],[13].

The load reduction control approach is described in detail by the authors in previous papers, and so only a brief summary is given here [1]. The controller functions as follows:

1. The blade root flapwise bending moments of the blades, M_{y1}, M_{y2}, and M_{y3}, are transformed into the fixed frame of reference using the inverse Coleman matrix. The transformation results in two variables in fixed coordinate systems, which are proportional to the rotor hub yaw-wise and tilt-wise moments. Essentially, the contributions of the blade loads to causing the entire rotor to yaw or tilt are calculated, and these variables are in fixed coordinates.

2. The transformed loads are used as inputs to a controller, and the control actions in the fixed frame are calculated. The system is approximated as LTI in the fixed frame, and because the yaw and tilt moments can be treated as independent signals, single input-single output (SISO) controllers can be used [5].

3. The control actions in the fixed frame are transformed into the rotating frame using the Coleman matrix. These are the demanded control actions of the TEFs or the blade pitch, and are the control inputs into Bladed.

Lastly, it should be mentioned that in the above formulation of the controller, the mean value (collective) TEF deployment angle is 0 degrees, initially. For the case of IPC, the collective blade pitch is used to control the rotor speed in above rated conditions, based simply on the baseline controller logic as if no individual pitch control actions were taking place. In the IFC case, the collective TEF deployment angle is an extra degree of freedom, which may be neglected by setting the value to 0 degrees at all times, or it can be used to augment rotor speed control by acting simultaneously with the standard controller collective pitch action. This possibility is discussed below.

2.2.3 Controller Implementation

For the IFC case, the deployment range of the TEFs is limited to ± 10 degrees, and the rate of change of the TEF deployment angle is limited to ± 40 degrees per second. The TEFs are used for load reduction across all operating ranges, including regions 2 and 3. The IPC controller is only utilized in above rated conditions (region 3), similarly to collective pitch control. The controller gains for IFC and IPC are detailed in the previous paper [1]; clearly the specific values of the gains are different for IFC and IPC, despite the identical controller structure.

As discussed previously, in the case of IFC the collective TEF angle is an extra degree of freedom, unused for load reduction. This flexibility can be exploited by using the collective TEF angle to also help control the rotor speed for power regulation in region 3, in order to augment the collective pitch angle that is used for this purpose, and potentially result in smoother power production and less wear on the pitch system. Thus, a simple proportional controller (P only) is used to control the collective TEF angle, with the generator speed error used as the input signal to the controller. The

collective TEF angle has a position limit of ±5 degrees, so as not to drown out the TEF deployment for load reduction.

This research does not aim to develop optimal control approaches to this problem, which is work for future investigations, and because system identification techniques are not utilized, stability of the system cannot be guaranteed. Instead, controllers that are easily implemented and achieve acceptable results are the goal, and the results indicate that this is indeed the case.

2.3 Simulations Run

Three categories of load cases are used to assess the performance of the various control approaches during these extreme events, and are summarized here. The IEC standards recommend a number of transient load cases, such as an "extreme operating gust" [15]; however, with the exception of the "normal stop during power production" case, these IEC gusts are not utilized. The IEC-recommended gusts occur in the presence of wind shear, tower shadow, and gravity loads, and these additional load sources, while realistic for an actual operating wind turbine, serve to drown out the loads produced solely by the gusts. As such, the true effects of the gusts, and the response of the various load reduction approaches, are not explicitly highlighted in these cases. In order to isolate the effectiveness of IFC and IPC at reducing the damage caused by gusts and extreme loads, simple step increases in the wind speed are utilized instead. These step functions occur over some specified period of time, in the absence of wind shear, tower shadow, gravity loads, and turbulence. While these load cases are extremely simple, and not particularly realistic, they are effective at illuminating the underlying physical effects of gusts and the corresponding response of the various control approaches. All simulations have a total length of 100 seconds, and in nearly all cases the SC, IPC, and IFC approaches are used.

1. Global Step Change, 15 m/s. The wind speed is initially constant at 15 m/s across the entire rotor. At some specified time, the gust occurs, increasing the wind speed to 20 m/s across the entire rotor. Thus, this is a global step change, as the gust occurs uniformly over the entire rotor, and not at specific locations within the rotor face. In essence, this type of gust simulates a very large scale eddy, with a characteristic length scale on the order of the rotor diameter or larger. The step increase in the wind speed occurs over several lengths of time: 0.5, 1.5, 3.0, 5.0, 7.5, and 10 seconds. The global step changes are depicted in Figure 1.

2. Local Step Change, 15 m/s. The wind speed is constant at 15 m/s across the entire rotor, except for certain points within the rotor face where the wind speed is 20 m/s. A 13 point by 13 point wind grid is used in these simulations. Only six points are potentially adjusted to values of 20 m/s, while the others always have values of 15 m/s. When looking at the rotor from upwind, these 6 points lie on the horizontal line at 3 o'clock, not including the center point of the grid. Figure 2 is useful for visualizing the situation. The 13 point by 13 point grid is shown, along with a circle representing the rotor face. Three specific local step

changes are considered. First, all six points on this line have values of 20 m/s. This encompasses the circle, square, and triangle points. Second, only the outer four points on the line have values of 20 m/s, and so only the square and triangle points. Finally, only the outer two points on the line have values of 20 m/s, and so only the triangle points. By adjusting these specific points in the wind input, a local gust is simulated. This approach allows for the effects of gusts at scales smaller than the rotor face to be examined.

3. Normal Stop during Power Production, 16 m/s (NS16). This load case is not the result of a gust, but instead it is a transient operational situation as the turbine is stopped at some point while it is producing power. The simulations use the wind input from the 16 m/s NTM simulation. 10 seconds into the simulation, the blades are pitched to 90 degrees at their maximum rate (8 degrees per second).

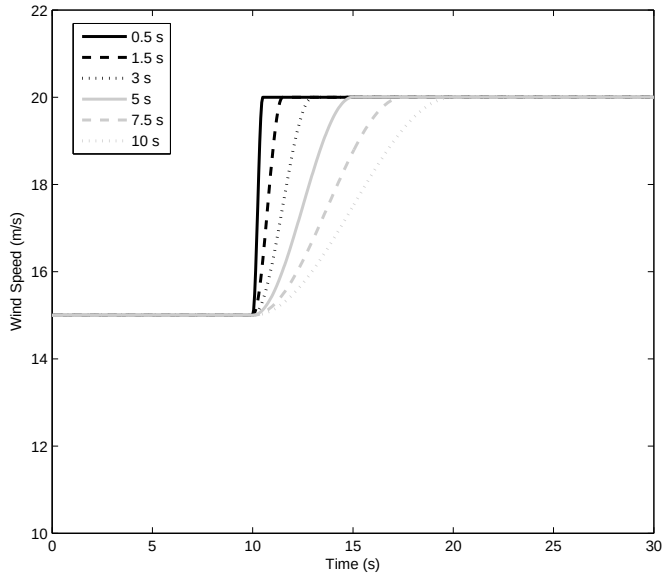

Figure 1: Time Series of Hub Height Wind Speeds for Global Step Changes

3 Extreme Loads Results and Discussion

The extreme load reductions are primarily calculated as the percent decrease in the range of the blade root flapwise bending moment, M_y, where the range is calculated as the difference between the maximum and minimum value of M_y. The range of M_y is labeled $R(M_y)$. The damage equivalent load of M_y, $DEQL(M_y)$, could also be used to quantify the loads during these extreme events; however, the changes in $R(M_y)$ or $DEL(M_y)$ for a

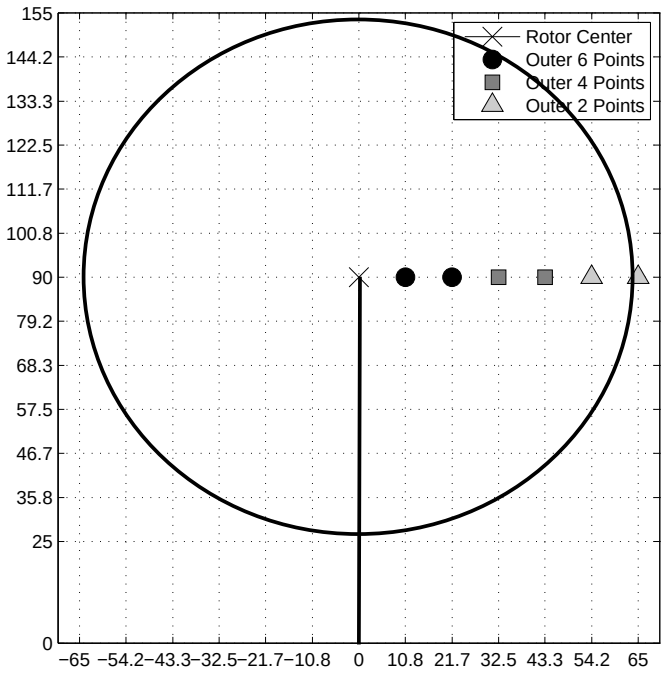

Figure 2: Time Series of Hub Height Wind Speeds for Global Step Changes

given load control approach are nearly identical, and $R(M_y)$ is more easily calculated. It should be emphasized that the global step change and local step change simulations both assume quasi-steady aerodynamic behavior. This is a potentially erroneous assumption, and it is evaluated later.

3.1 Global Step Change

The values of $R(M_y)$ for the various control approaches and global step change lengths are shown in Table 1. The percent difference in $R(M_y)$ when using either IFC or IPC is also calculated and shown in Table 1.

Table 1 indicates:

- IFC is effective at reducing $R(M_y)$ for all gust lengths. Specifically, $R(M_y)$ is decreased only slightly for very rapid gusts, i.e. gust lengths of 0.5 and 1.5 seconds. For less rapid gusts occurring over 3 seconds or longer, the reductions in $R(M_y)$ are significant, with an average value of approximately 8%. This improved performance for longer gust lengths is explained below.

- It appears that IPC has a negligible effect on $R(M_y)$ for all gust lengths. A physical explanation for these results is presented below as well.

	SC	IFC		IPC	
Step Length (s)	$R(M_y)$ $[Nm * 10^6]$	$R(M_y)$ $[Nm * 10^6]$	Change [%]	$R(M_y)$ $[Nm * 10^6]$	Change [%]
0.5	6.91	6.76	**-2.2%**	6.92	**0.1%**
1.5	6.42	6.17	**-4.0%**	6.44	**0.3%**
3.0	5.46	5.11	**-6.5%**	5.47	**0.1%**
5.0	4.35	3.92	**-9.7%**	4.36	**0.3%**
7.5	4.03	3.69	**-8.6%**	4.03	**-0.2%**
10.0	3.48	3.22	**-7.5%**	3.45	**-1.0%**

Table 1: Load Reductions for Global Step Change

- Once again, it is important to note that the simulations operate under the assumption of quasi-steady aerodynamic behavior. The rapid change in the wind speed during these simulations may in fact lead to unsteady aerodynamic effects.

Investigating the time series from these simulations helps to better understand the results shown in Table 1. Figure 3 shows the time series of M_y for blade 1 for all three control approaches (SC, IFC, and IPC), the blade pitch for the SC and IPC cases, and the TEF behavior for the IFC case. The time series are shown for both the 1.5 second gust length and the 5 second gust length.

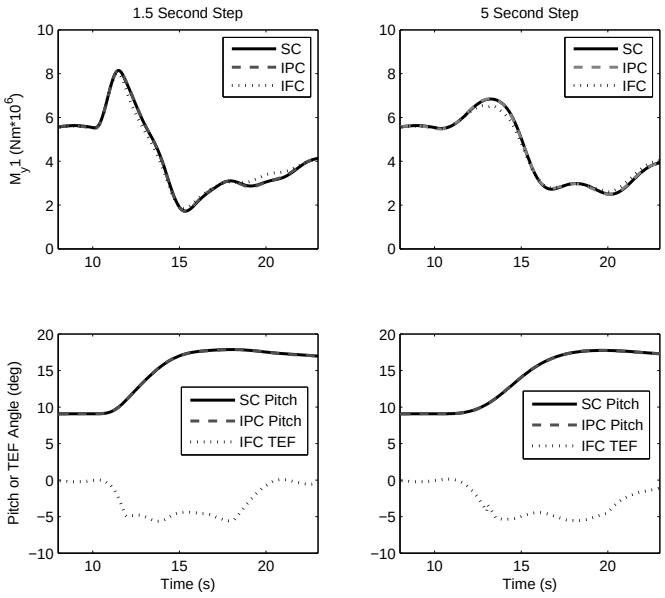

Figure 3: Global Step Change Time Series Results

Figure 3 indicates:

- M_y and the blade pitch are virtually identical for the SC and IPC cases, and in fact are indistinguishable in Figure 3, i.e. the black and dashed gray lines are exactly on top of each other. This confirms the negligible change in $R(M_y)$ shown in Table 1. Clearly, despite the rapid change in the wind speed and the blade loads, the blade pitch does not respond to reduce M_y in the IPC case.

- On the other hand, for both SC and IPC, the blade pitch does increase during the gust (it also increases in the IFC case, which is not shown). This increase is a result of using the collective pitch angle for rotor speed control in above rated conditions. As the wind speed increases during the gust, the rotor speed increases, and so the collective pitch angle is also increased to reduce the aerodynamic torque on the rotor and reduce the speed to the rated value.

- For both gusts, IFC does in fact reduce the peaks in the M_y signal. The reduction is noticeably larger for the 5 second gust.

- During the gust, and for some time after the gust has finished, the TEF deflection is approximately constant at -5 degrees. For the rest of the simulation, the TEF deflection is approximately 0 degrees. In fact, the TEF behavior mirrors the blade pitch behavior: the collective TEF deflection is being used to control the rotor speed during the gusts. As described previously, when using IFC, the TEFs are also utilized to control the rotor speed in above rated conditions, and the collective TEF deflection angle is limited to ± 5 degrees. Thus, since the gust causes the rotor speed to increases, the TEFs collectively deploy to a negative value to help slow the rotor down. Moreover, this indicates that the TEFs are not behaving so as to explicitly reduce the loads on the blades.

These results lead to an important conclusion regarding both IFC and IPC: during these types of gusts, despite the substantial changes in the blade loads (M_y), neither the TEFs nor the blade pitch explicitly respond to reduce the loads. This result initially appears curious, but in fact it is a direct function of two factors: the control architecture that is employed and the nature of the gusts that are utilized.

1. The blade root flapwise bending moments are transformed into non-rotating coordinates using the Coleman matrix, which then yields the tilt and yaw moments on the fixed rotor hub. For both IFC and IPC, the response of either the TEFs or the blade pitch aims to minimize these tilt and yaw moments. As the results of the fatigue load simulations indicate ([1]), this is an effective approach for reducing the blade loads. However, it must be emphasized that the explicit objective of this particular control architecture is not to reduce the blade loads directly, but instead to minimize the tilt and yaw moments, which then leads to reduced blade loads in most cases.

2. The gusts used in these simulations are "global" gusts, as the wind speed is uniform across the rotor face. As such, this type of gust does not generate a sizable tilt or

yaw moment on the rotor hub. The forces increase approximately equally on each blade, and so while the bending moments at the blade roots increase, the tilt and yaw moments do not increase appreciably when the gust is this global type.

When these two factors are considered together, it becomes clear why neither IFC nor IPC react to reduce the blade loads. A global gust, which is uniform across the rotor face, generates very little tilt or yaw moment on the rotor hub, and so for the control architecture employed in this research, the TEFs or the blade pitch do not respond to reduce the blade loads.

The decrease in $R(M_y)$ that occurs in the IFC simulations is a result of using the collective TEF deployment for controlling the rotor speed in above rated conditions. The resulting decrease in the blade loads is an ancillary benefit of this use of the TEFs; it is not the explicit goal of using the collective TEFs but instead is a secondary effect. This reduction in $R(M_y)$ should not be discounted however. A substantial reduction in the blade loads is possible during these global gusts as long as the collective TEF deployment is utilized for controlling the rotor speed. It is also now clear why the load reductions are larger for the 5 second gust than the 1.5 second gust. For the faster 1.5 second gust, the TEFs are not fully deployed collectively to -5 degrees until approximately 2 seconds after the gust begins, and so the loads are not significantly reduced during the gust itself. Essentially, the gust occurs so quickly that by the time the TEFs are collectively deployed to control the rotor speed, the transient portion of the gust has finished. For the 5 second gust, the TEFs are fully deployed collectively to -5 degrees approximately 3 seconds after the gust begins, and so they are able to affect the loads during the gust itself. The result is the peak of M_y is reduced appreciably during this slower gust.

Overall, these results help highlight some of the limitations of the control architecture that is utilized in this research. Specifically, the explicit goal of the controller is not blade loads reduction, but instead to minimize the tilt and yaw moment on the rotor hub. While this goal leads to reduced blade fatigue loads the majority of the time, there are also instances, such as gusts with spacial scales on the order of the rotor diameter or larger, in which the control architecture is ineffective. Other control approaches, perhaps those that utilize the measured blade loads directly, or those that also attempt to add damping to the tower fore-aft motion, may be more effective during these large scale gusts.

It should be noted that in below rated conditions, during global gusts, IFC would be equally ineffective compared to the SC and IPC approaches. That is, in below rated conditions, the collective TEF deployment angle is not utilized, and so the blade loads are unchanged compared to SC, because the global gust generates very little tilt or yaw moment. On the other hand, it is debatable if it would even be desirable to reduce the blade loads during gusts in below rated conditions. When a gust occurs, the rotor speeds up to capture as much energy from the wind as possible. If the TEFs were deployed to reduce the loads on the blades during gusts, they would also act to retard the increase in rotor speed, and therefore reduce the power extracted from the wind.

Finally, any type of gust that is uniform across the rotor face is likely to produce similar results. The IEC-type gusts are no exception, as all uniform gusts do not produce

sizable tilt or yaw moments, and therefore no explicit load reduction action takes place.

3.2 Local Step Change

For the local step change simulations, each time the blade passes through the localized region of higher wind speed, it experiences a gust. As such, for a 100 second simulation, each blade will experience this local gust twenty times. The results are consolidated as follows. First, the maximum value of M_y is determined each time the local gust occurs, yielding twenty values. Next, the difference between each maximum value and the average value of M_y during the entire simulation is calculated. Finally, the average for the twenty differences is computed. In sum, the average difference between the maximum value of M_y during each gust and the average value of M_y during the entire simulation is calculated. This is essentially a calculation of the average value of $R(M_y)$ for each gust, except that the average value of M_y is used instead of the minimum value. The average value is used because it is constant for each control approach utilized, whereas the minimum value differs somewhat. In general, however, the difference is small, and the distinction is made here only for completeness. $R(M_y)$ is used to label the results once again, even though it is calculated differently.

The values of $R(M_y)$ for the various control approaches and the number of altered wind grid points are shown in Table 2. The percent difference in $R(M_y)$ when using either IFC or IPC is also calculated.

	IFC	IPC
Number of Local Wind Grid Points	Change [%]	Change [%]
2	**-15.4%**	**0.1%**
4	**-15.0%**	**-8.7%**
6	**-15.2%**	**-10.5%**

Table 2: Load Reductions for Local Step Change

Table 2 indicates:

- For all three local gusts, IFC results in substantial reductions in $R(M_y)$. The reductions in $R(M_y)$ are essentially constant at approximately 15%.
- For IPC, $R(M_y)$ is reduced sizably when 6 points of the wind grid are altered (although not as much as IFC), but the ability to reduce $R(M_y)$ worsens as the number of altered points is reduced.
- Once again, it is important to note that the simulations operate under the assumption of quasi-steady aerodynamic behavior. The rapid change in the wind speed during these simulations may in fact lead to aerodynamic behavior that is not quasi-steady.

These results clearly indicate an important distinction between IFC and IPC, namely the bandwidth of the two load control approaches. As the number of altered points in the wind grid is decreased, the scale of the local gust is decreased as well. Moreover, the effects of the gust are felt by the blade over a shorter period of time. When all 6 points in the wind grid are altered, a passing blade is affected by the gust for approximately 2.5 seconds. In the case of 4 altered points, this value is reduced to approximately 0.8 seconds, and for 2 altered points it it only approximately 0.4 seconds. Because IFC has significantly higher bandwidth than IPC, the ability to reduce the local gusts appears to be independent of the scale of the local gust. In contrast, the effectiveness of IPC is highly dependent on the scale of the local gust. Overall, these results indicate a clear advantage of using IFC compared to IPC.

The distinction between these local gusts and the global gusts discussed above should also be emphasized. The global gusts are uniform across the rotor face, and therefore produce very little changes in the tilt and yaw moments on the rotor. In contrast, the local gusts, which occur solely on one blade, do indeed produce a yaw or tilt moment. For the specific location of the local gusts used in these simulations, a yaw moment is produced. More generally, a local gust produced on a blade must generate a tilt or yaw moment, and so the load control approaches, whether IFC or IPC, indeed react and reduce the blade loads.

Once again the time series from these simulations are utilized to better understand the results shown in Table 2. Figure 4 shows a 3 second window of the time series of M_y for blade 1 for all three control approaches (SC, IFC, and IPC), the blade pitch for the SC and IPC cases, and the TEF behavior for the IFC case. The time series are shown for the cases when 2 and 6 local wind data points are altered.

Figure 4 indicates:

- The length of time that the blade is affected by the local gust is clearly highlighted, as the gust when only 2 points are altered occurs over a significantly shorter period of time than when 6 points are altered. As a result, the loads are increased more when 6 points are altered, as the blade has a longer time to feel the effect of the increased wind speed.

- The TEFs behave similarly for either IFC simulation, and clearly act to reduce the loads on the blades during the local gust. The range of deployment is fairly small, approximately ± 3 degrees. This response of course depends on the gains used for the controller.

- For IPC, the blade pitch has a negligible reaction when 2 local points are altered, and a very small reaction when 6 points are altered. The slow reaction of the blade pitch is clearly highlighted in these time series.

In sum, when local gusts on the scale of the blade or smaller occur, the load control approaches display vastly different behavior and effectiveness. The significantly higher bandwidth of IFC appears to be a valuable asset during these local gusts, and an important advantage relative to IPC.

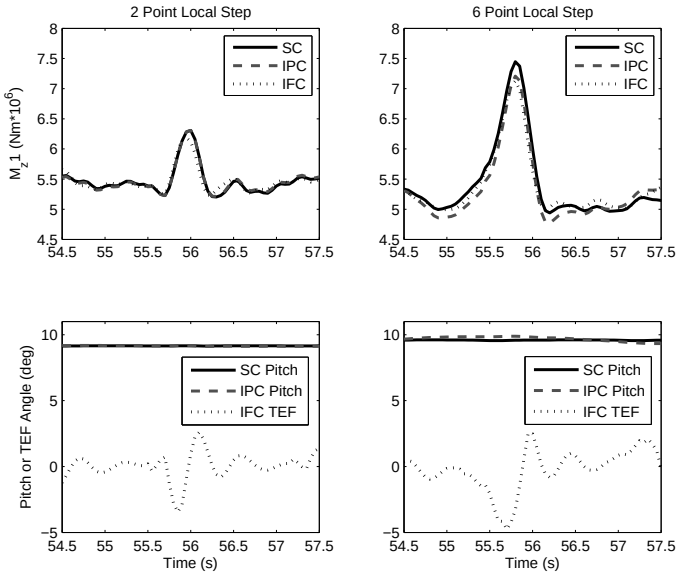

Figure 4: Local Step Change Time Series Results

3.3 Normal Stop during Power Production

The IEC standards recommend simulating a load case in which the rotor is brought to a stop while it is producing power [15]. The 16 m/s NTM wind input is used for these simulations. After 10 seconds of power production, the blades are pitched to their maximum feathered value of 90 degrees, at the maximum rate of 8 degrees per second. Because the blade pitch is used exclusively for braking the rotor, IPC is not a viable load control approach during normal stop situations. Thus, only IFC is compared to SC here. Once again, $R(M_y)$ is used to quantify the loads on the blades, and it is defined in the same way as section 3.1. The values of $R(M_y)$ for the SC and IFC are shown in Table 3. The percent difference in $R(M_y)$ when using IFC is also calculated.

	SC	IFC	
Load Case	$R(M_y)$ $[Nm * 10^6]$	$R(M_y)$ $[Nm * 10^6]$	Change [%]
NS16	9.53	9.26	**-2.8%**

Table 3: Load Reductions for NS16

Table 3 indicates a fairly minor reduction in $R(M_y)$ when utilizing IFC. By investigating the time series of M_y during this normal stop, a better understanding of the results can be obtained. Figure 5 shows the time series M_y for both the SC and IFC cases, as well as the TEF behavior. Not surprisingly, based on the results of Table 3,

there is essentially no difference in M_y between the two simulations.

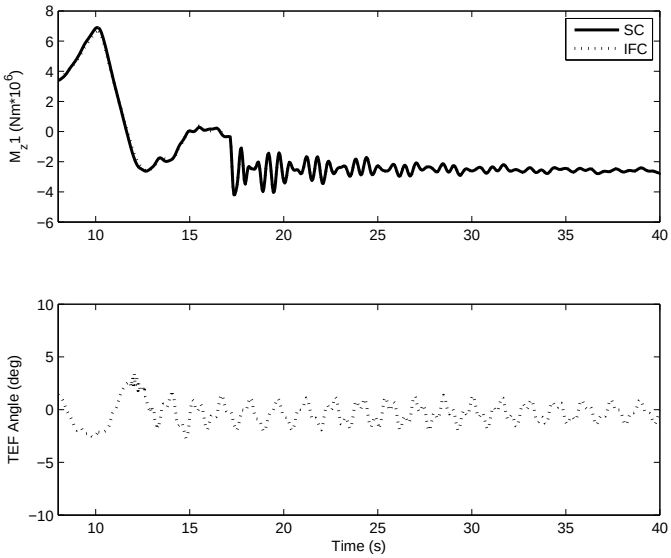

Figure 5: Normal Stop during Power Production Results

There is a basic physical explanation for the relative ineffectiveness of IFC during these simulations. The deflection of the TEFs results in changes in the lift on the blade section (and only minor changes in the drag during attached flow conditions). As the blades are pitched towards feather during the normal stop, the rotor slows down, and so the direction of lift is predominantly in the in-plane direction. This is in contrast to normal operating conditions, when the lift direction is mostly in the out of plane direction. The TEFs respond to changes in the flapwise bending moment, which is indeed in the out of plane direction. Thus, as the blades pitch to feather, the TEFs have a significantly reduced ability to control out of plane loads, and therefore reduce M_y. While this investigation into shut downs and safety systems is preliminary, it does seem to indicate that the use of TEFs and other load control approaches is relatively ineffective during these events, at least compared to the load reductions that are attainable during normal power production conditions and gusts.

4 Limitations of Results

The Bladed simulations rely on a number of assumptions, and it is important to justify some of these to help establish the validity of the results. In particular, the assumption of quasi-steady aerodynamics is assessed. During the simulations, Bladed assumes quasi-steady aerodynamic behavior of the airfoil sections. That is, during operation as the angle of attack of an airfoil section changes and as the TEF deflects to control loads, the

aerodynamic performance of the airfoil, characterized by C_L, C_D, and C_M, is determined directly from the airfoil tables that are input into Bladed. Thus, the aerodynamic performance is calculated in a quasi-steady manner, by assuming that C_L, C_D, and C_M change with each time step dependent solely on the values of α and the TEF deployment angle, and not on how quickly these parameters are changing.

In reality, the aerodynamic performance of the airfoil sections responds to changes in α and the TEF deployment angle in a dynamic sense. A rapid change in the angle of attack does not result in an instantaneous change in C_L, C_D, and C_M; instead, C_L, C_D, and C_M change over some period of time until they reach a steady state value. Leishman provides a detailed look at unsteady aerodynamic behavior for a rotor [16]. Only when the angle of attack and the TEF deployment angle are changing slowly enough is the assumption of quasi-steady aerodynamics a valid approximation.

When an airfoil section experiences some disturbance, the degree of unsteadiness caused by that disturbance can be quantified by the reduced frequency, k. k is a non-dimensional parameter, and is determined using Eq. 1, where c is the local chord length of the section, U is the local relative velocity at the section, and ω is the frequency of the disturbance, in units of radians per second [16].

$$k = \frac{c}{2U}\omega \tag{1}$$

The larger the value of k, the more the actual performance of the airfoil deviates from the performance when one assumes quasi-steady behavior. As a general rule, when $k < 0.05$ the aerodynamics can be considered quasi-steady, and when $k > 0.05$ they are considered unsteady.

The issue of unsteady aerodynamics is particularly important in the context of smart rotor control. For very rapid changes in the inflow conditions, and therefore in the loads, there is a phase delay between the actual disturbance and the aerodynamic response of the airfoil section, and so the loads. Since the load reduction controllers, using IFC or IPC, respond to the measured blade loads, the response of the controllers is therefore delayed when the disturbance occurs very rapidly, and so the load mitigation abilities are reduced.

The extreme load simulations are analyzed to assess the possible effects of assuming quasi-steady aerodynamic behavior. For each global gust, a simple analytic method is utilized to quantify the degree of unsteadiness in the simulations, and approximate the reduced frequency. The global gusts are shaped similarly to the first quarter of a sine wave, i.e. the first 90 degrees. The TEF behavior during the global gust shows a similar shape, as does the angle of attack. It is therefore assumed that the global gust represents the first fourth of a sinusoidal variation in the wind speed, the TEF deflection, and the angle of attack. As such, the frequency, ω, used to calculate k in Eq. 1 is simply the inverse of four times the global step length. So, for a 0.5 second gust, the period of the disturbance is assumed to be 2 seconds, and so the frequency is 0.5 Hz, or 3.14 radians per second. For a 10 seconds gust, the frequency is only 0.157 radians per second. Next, k is calculated for the blade station $r = 52.75\ m$, with $c = 2.518\ m$ and U taken as the average relative wind speed during the simulation, which is approximately 70 m/s

in every case. The results are shown in Figure 6, which shows the computed values of k as a function of the global step length.

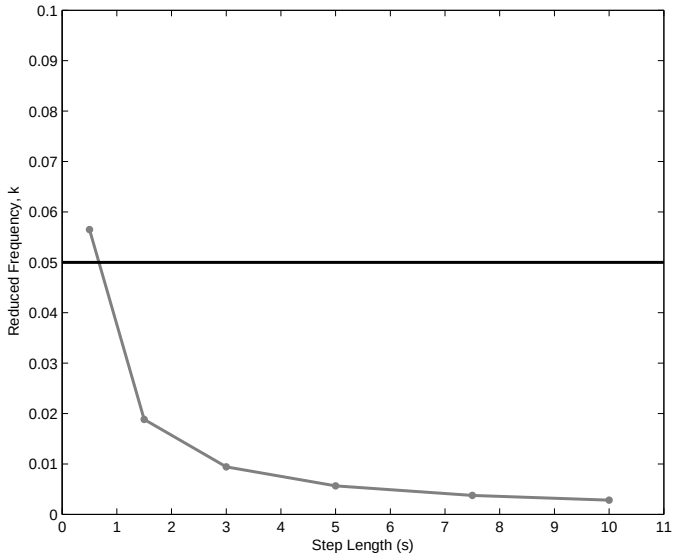

Figure 6: Evaluation of Unsteadiness for Global Gust

Figure 6 clearly indicates that k decreases as the global step length increases. This is logical, as a slower gust should indeed result in behavior that is closer to quasi-steady than a faster gust. Moreover, with the exception of the 0.5 second step length, k is less than 0.05 in all cases, and therefore these instances appear to be quasi-steady in nature. Even for the 0.5 second step, the value of k is approximately 0.057, and so it is only slightly greater than 0.05. Thus, with the exception of the 0.5 second step change in the wind speed, the results of the global gust simulations appear to be such that assuming quasi-steady aerodynamic behavior is indeed a valid assumption, and so the results can be trusted. Again, this is a simple and approximate approach to evaluating the unsteadiness of the aerodynamics, but it does help indicate whether or not the assumption of quasi-steadiness is valid.

The local gusts are evaluated as well, to determine the validity of the assumption of quasi-steady aerodynamic behavior. The reduced frequency is approximated in a similar manner as the global gusts. For the local gusts, the time series indicate that TEF deflection angle executes essentially one full cycle during each local gust. That is, the TEF deflection resembles a sine wave during each local gust, and so does the angle of attack. Thus, the period of each local gust is used to calculate the frequency of the disturbance and therefore the reduced frequency k. As with the global gust, k is calculated for the blade station $r = 52.75\ m$, with $c = 2.518\ m$ and U taken as the average relative wind speed during the simulation, which is approximately 69 m/s in

every case. The results are shown in Figure 7, which shows k as a function of the number of altered wind grid points.

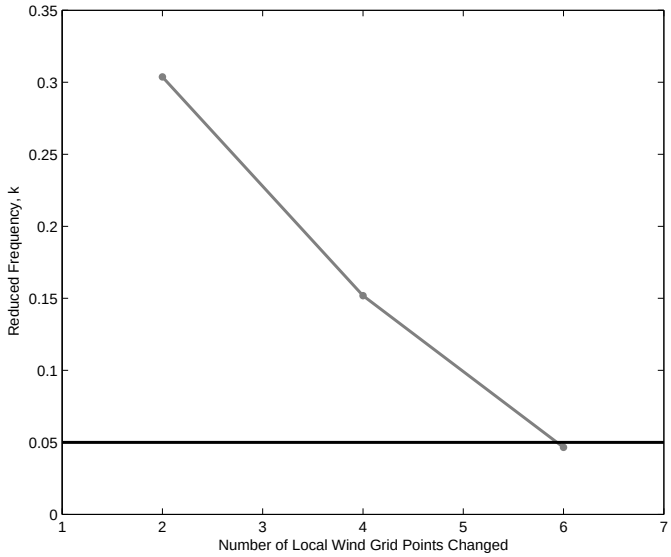

Figure 7: Evaluation of Unsteadiness for Local Gust

Figure 7 indicates that using this method to estimate the unsteadiness of the gust results in potentially very large values of k. In fact, only in the case where 6 of the wind grid points are altered, which is a larger special gust, is the value of k less than 0.05. For the other two cases, k is significantly larger than 0.05, indicating a highly unsteady situation. While this method for calculating k is simple and approximate, it appears to indicate that the results may be invalid when only 2 or 4 wind grid points are altered. On the other hand, the results when 6 wind grid points are altered appear to be valid, and the conclusions drawn from these results are likely sound. Namely, IFC is more effective at reducing the effects of small scale gusts, with characteristic length scales on the order of the blade length or less.

Finally it should be noted that for all evaluations of unsteadiness, the degree of unsteadiness depends strongly on the spanwise blade section under consideration. The inboard sections, where the chord length is larger and the relative wind speed is smaller, have larger reduced frequencies. However, there are no TEFs on these sections, and so any errors due to unsteady aerodynamic effects will be constant across all the simulations. It is only on the TEF section where the simulations may differ in terms of unsteady aerodynamic behavior.

5 Conclusions

The primary goal of smart rotor control is to reduce fatigue loads on the blades, and the controller used in this research is designed for this purpose. However, extreme loads caused by gusts and other transient operations also cause damage in wind turbines, and it is important to determine if smart rotor control approaches can be effective during these situations as well. This research investigates the performance of smart roto0r control approaches, designed for fatigue load reduction, during extreme load events. The major conclusions of this research are:

- The control approach utilized for fatigue load reductions, namely the multi-blade transformation, is ineffectual at reducing the blade loads during large scale global gusts. These gusts do not produce sizable yaw or tilt moments, and so the response of IFC or IPC is minimal.
- The use of the trailing edge flaps for rotor speed control in above rated conditions has the ancillary benefit of reducing blade loads. This is a secondary effect, but valuable nonetheless.
- For small scale gusts, the significantly higher bandwith of TEFs results in superior load reduction compared to IPC.
- During safety situations when the blades are pitched to feather, the current load reduction approach using TEFs is no longer effective, as the direction of lift rotates from predominantly the out of plane direction to the in plane direction.
- Unsteady aerodynamics are a potentially relevant effect during gusts, and the degree of unsteadiness in a simulation should be assessed. While most results from the simulations appear valid, some should be qualified due to large reduced frequencies.

Acknowledgments

The authors would like to acknowledge STW for funding this research, and Ervin Bossayni, Thanasis Barlas, and Jan-Willem van Wingerden for their contributions.

References

[1] Lackner, M. and van Kuik, G. (2009) A comparison of smart rotor control approaches using trailing edge flaps and individual pitch control. *47th AIAA Aerospace Science Meeting and Exhibit*.

[2] Barlas, T. (2006) Smart rotor blades and rotor control for wind turbines: State of the art. Knowledge base report for upwind wp 1b3, Delft University Wind Energy Research Institute (DUWIND).

[3] Barlas, T. and van Kuik, G. (2007) State of the art and prospectives of smart rotor control for wind turbines. *The Science of Making Torque from Wind, Journal of Physics: Conference Series*.

[4] van Engelen, T. and van def Hooft, E. (2005) Individual pitch control inventory. Tech. rep., Technical University of Delft.

[5] Bossayni, E. (2003) Individual blade pitch control for load reduction. *Wind Energy*, **6**.

[6] Selvam, K. (2007) *Individual Pitch Control for Large Scale Wind Turbine*. Master's thesis, Technical University of Delft.

[7] Andersen, P., Henriksen, L., Gaunaa, M., Bak, C., and Buhl, T. (2008) Integrating deformable trailing edge geometry in modern mega-watt wind turbine controllers. *2008 European Wind Energy Conference and Exhibition*.

[8] McCoy, T. and Griffin, D. (2006) Active control of rotor aerodynamics and geometry: Statues, methods, and preliminary results. *44th AIAA Aerospace Science Meeting and Exhibit*.

[9] Zayas, J., van Dam, C., Chow, R., Baker, J., and Mayda, E. (2006) Active aerodynamics load control for wind turbine blades. *European Wind Energy Conference*.

[10] Jonkman, J., Butterfield, S., Musial, W., and Scott, G. (2008) Definition of a 5-mw reference wind turbine for offshore system development. TP 500-38060, National Renewable Energy Laboratory.

[11] Troldborg, N. (2005) Computational study of the risøb1-18 airfoil with a hinged flap providing variable trailing edge geometry. *Wind Engineering*, **29**, 89–113.

[12] Drela, M. and Youngren, H. *XFOIL 6.9 User Primer*. MIT.

[13] Bir, G. (2008) Multi-blade coordinate transformation and its application to wind turbine analysis. *46th AIAA Aerospace Science Meeting and Exhibit*.

[14] Coleman, R. and Feingold, A. (1958) Theory of self-excited mechanical oscillations of helicopter rotors with hinged blades. Tech. rep., NASA.

[15] *IEC 61400-1 Ed.3: Wind turbines - Part 1: Design requirements*.

[16] Leishman, J. .